ELSEVIER

Journal of Alloys and Compounds 271–273 (1998) 437–443

Journal of ALLOYS AND COMPOUNDS

Transport properties of $(U_{1-x}Np_x)Pd_2Al_3$ and $(U_{1-x}Pu_x)Pd_2Al_3$ intermetallic solid solutions

F. Wastin*, E. Bednarczyk, J. Rebizant

European Commission, Joint Research Centre, Institute for Transuranium Elements, Postfach 2340, D-76125 Karlsruhe, Germany

Abstract

We present and summarize the first characterization of the physical properties of $U_{1-x}Np_xPd_2Al_3$ and $U_{1-x}Pu_xPd_2Al_3$ solid solutions (with $0.005 \leq x \leq 0.9$) obtained by resistivity measurements (between 1.4 and 300 K). For very low Np doping ($x=0.005$) a superconducting transition is still observed at 1.5 K, whereas for $x \geq 0.01$ this transition is absent or shifted below our temperature range. The doping effects on the magnetic and Kondo lattice behaviors of UPd_2Al_3 are discussed. © 1998 Elsevier Science S.A.

Keywords: $U_{1-x}Np_xPd_2Al_3$; $U_{1-x}Pu_xPd_2Al_3$; Resistivity

1. Introduction

Heavy-fermion superconductor (HFS) materials have attracted much attention due to their unconventional superconducting and magnetic properties. Most of these materials are Ce- or U-based intermetallic compounds. It is now well-established that the f electrons play a central role in these unusual properties. This has, therefore, stimulated the study of the related transuranium compounds [1].

Since UPd_2Al_3 was reported as the highest T_c HFS [2], recent works have been devoted to its homologue Np and Pu compounds [3–5].

On the other hand, in a new attempt to shed light on the ground state and intersite correlations of the f electron in UPd_2Al_3, a number of investigations have been made on the effects of alloying substitution on the Pd, Al or U sites [6–9]. These last studies were mainly carried out with Y, Pr, Gd or Th substitutions.

It seemed interesting to study the Upd_2Al_3–$NpPd_2Al_3$ solid solution system where a complete range of solubility is observed. Previous studies of this system by Np-Mössbauer spectroscopy and resistivity measurements have already been reported [4,10,11]. We have extended these studies by considering very low dilution on the uranium site by Np (<1% Np) and started to investigate a homologue series by diluting with the non-magnetic Pu compound. Resistivity measurements of both series $U_{1-x}An_xPd_2Al_3$ (with An=Np or Pu) are presented and compared.

2. Experimental details

The solid solutions were prepared by arc melting stoichiometric amounts of the pure compounds previously obtained. They were then characterized by X-ray diffraction, metallography and microprobe analysis as presented in another contribution to this conference [12]. No further thermal treatment was found to be necessary.

Resistivity measurements on encapsulated bulk samples were performed down to 1.4 K with a conventional four-probe a.c. method. Because of the dimensional uncertainties, the probable presence of microcracks and the preferential orientation of the crystallites in the bulk samples, the absolute resistivity values have not been considered here.

3. Results and discussion

A $PrNi_2Al_3$-type structure was observed in the whole range of concentration with the lattice parameters listed in Table 1.

The Fig. 1 Fig. 2 Fig. 3 Fig. 4 show the resistivity ratio $\rho/\rho_{300\ K}$ curves on a logarithmic scale of temperature, obtained for each system on polycrystalline samples.

*Corresponding author. Tel.: +49 7247 951387; fax: +49 7247 951590; e-mail: wastin@itu.fzk.de

0925-8388/98/$19.00
PII: S0925-8388(98)00106-6

Table 1
Lattice parameters of $U_{1-x}An_xPd_2Al_3$ compounds and characteristic temperatures of the anomalies observed in their resistivity

Compound	a (pm)	c (pm)	T_c (K)	T_N (K)	$T\rho_{max}$ (K)
UPd_2Al_3	536.5(1)	418.9(1)	1.9	14.2	85
$U_{0.995}Np_{0.005}Pd_2Al_3$	536.6(1)	418.7(1)	1.5	14.0	85
$U_{0.99}Np_{0.01}Pd_2Al_3$	536.9(1)	419.1(1)	—	13.5	85
$U_{0.99}Pu_{0.01}Pd_2Al_3$	537.1(1)	419.2(1)	—	14.0	85
$U_{0.97}Np_{0.03}Pd_2Al_3$	537.2(1)	419.2(1)	—	13.0	75
$U_{0.92}Np_{0.08}Pd_2Al_3$	537.1(1)	419.1(1)	—	11.4	80
$U_{0.9}Np_{0.1}Pd_2Al_3$	536.9(1)	419.1(1)	—	10.5	55
$U_{0.9}Pu_{0.1}Pd_2Al_3$	537.1(1)	419.3(1)	—	10.0	50
$U_{0.7}Np_{0.3}Pd_2Al_3$	537.5(1)	419.2(1)	—	4.5	7
$U_{0.7}Pu_{0.3}Pd_2Al_3$	537.9(1)	419.5(1)	—	—	—
$U_{0.5}Np_{0.5}Pd_2Al_3$	538.0(1)	419.3(1)	—	5.5	40
$U_{0.5}Pu_{0.5}Pd_2Al_3$	538.4(1)	419.7(1)	—	—	—
$U_{0.2}Np_{0.8}Pd_2Al_3$	538.7(1)	419.6(1)	—	37/22	135
$U_{0.2}Pu_{0.8}Pd_2Al_3$	539.8(1)	420.0(1)	—	—	—
$NpPd_2Al_3$	539.2(1)	419.5(1)	—	38/24	145
$PuPd_2Al_3$	540.3(1)	420.2(1)	—	—	—

Characteristic temperatures are listed in Table 1. In the following sections, we divide the discussion of these curves according to the An (Np or Pu) content.

3.1. Very low range of An content, $0 \le x \le 0.03$

Shown in Fig. 1 are the resistivities versus the temperature for $U_{1-x}An_xPd_2Al_3$ (with An=Np or Pu and $x \le 0.03$). The resistivity curve obtained for our pure Upd_2Al_3 compound is in very good agreement with previous reported data [1,13]. The overall behavior of the doped samples is very similar to the pure one. As the temperature is lowered, we observe a Kondo-like increase, followed by a broad maximum, characteristics for Kondo lattices, and a rapid decrease. In the temperature range from 300 to 150 K, the experimental data are well fitted with a

$$\rho = a - b \cdot \ln T \quad (1)$$

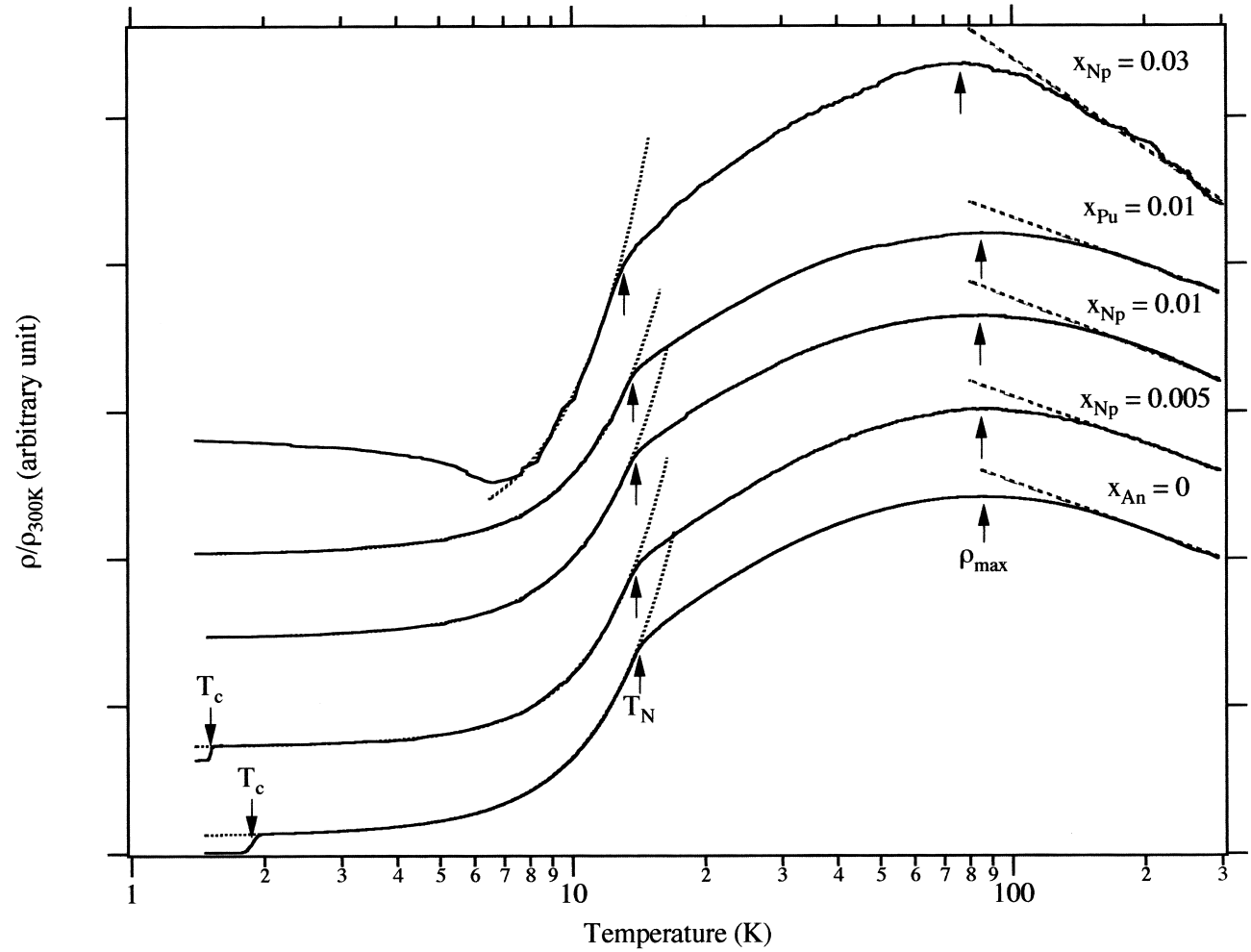

Fig. 1. Normalized resistivity $\rho/\rho_{300\ K}$ vs. a logarithmic scale of T, of $U_{1-x}An_xPd_2Al_3$ compounds. Curves are displaced for clarity. Arrows point out characteristic temperatures, as indicated in Table 1, and dashed lines show results of calculation as described in the text.

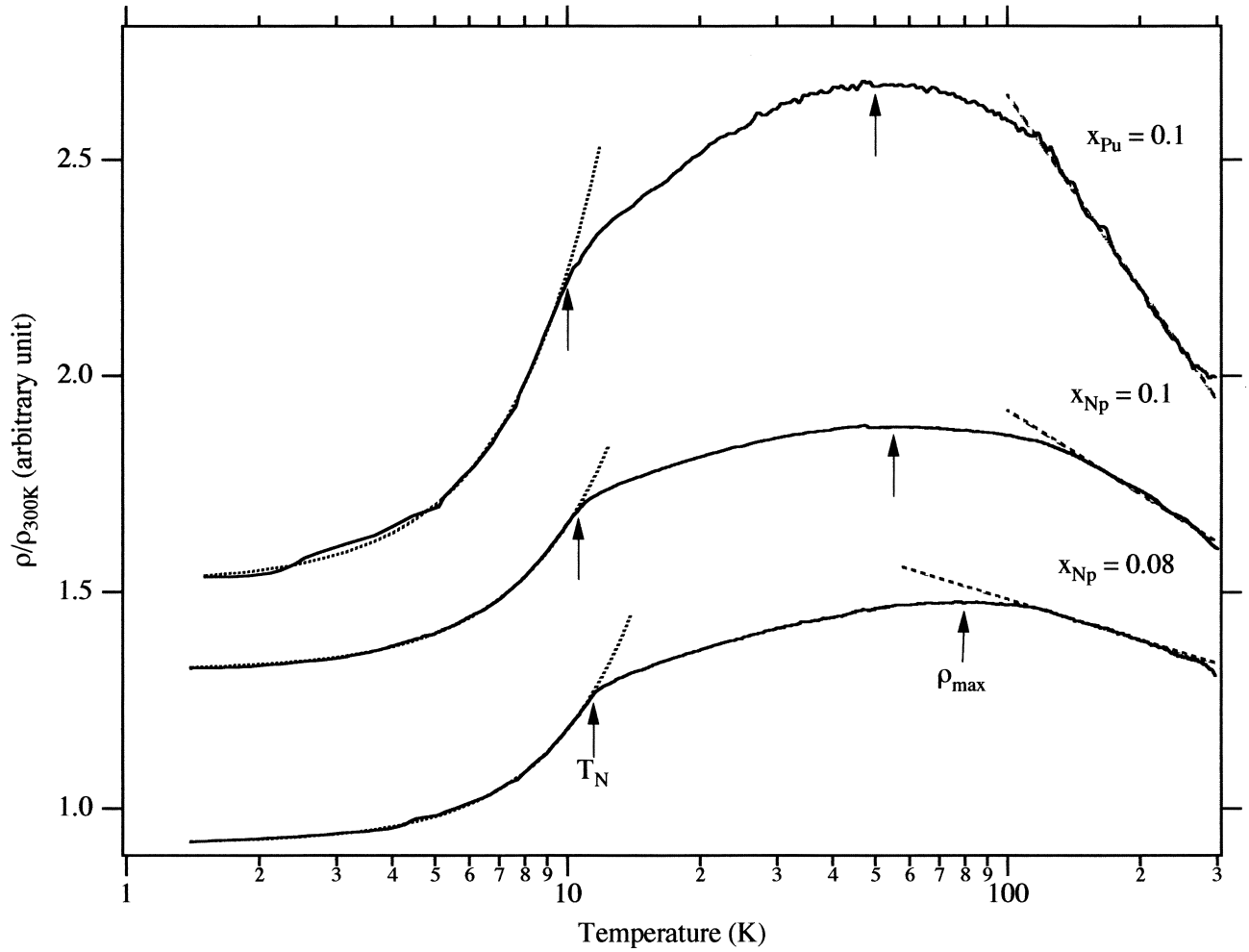

Fig. 2. Normalized resistivity $\rho/\rho_{300\ K}$ vs. a logarithmic scale of T, of $U_{1-x}An_xPd_2Al_3$ compounds. Curves are displaced for clarity. Arrows point out characteristic temperatures, as indicated in Table 1, and dashed lines show results of calculation as described in the text.

type law and, up to 1% doping, no significant difference in the fit parameters is observed. A typical value of b/a of about 0.10 is obtained (see Table 2). For 3% Np a pronounced increase of the slope (b/a is about 0.13) may suggest that the Kondo temperature decreases with increasing x, and is corroborated by the decrease of the temperature of the resistivity maximum (see arrows on Fig. 1 and Table 1).

Below 30 K, there is an abrupt and large decrease in $\rho(T)$ around 14 K due to the onset of a long-range antiferromagnetic ordering. The ordering temperature T_N is only slightly decreased by An doping, as presented in Table 1. Below T_N, an excellent fit (dashed line in Fig. 1) to the experimental data can be achieved using the sum of an expression appropriate for an antiferromagnet with an energy gap and a T^2 term [14], reflecting Fermi-liquid behavior,

$$\rho = \rho_0 + cT[1 + 2T/\Delta]\exp(-\Delta/T) + AT^2 \quad (2)$$

with the parameters, normalized to the respective $\rho_{300\ K}$ value, as listed in Table 2 (an estimation of the absolute value of these parameters may be obtained by considering a typical value for $\rho_{300\ K}$ of 200 $\mu\Omega\cdot$cm).

At low temperature, a superconducting transition is still observed for 0.5% doping Np but already shifted to 1.5 K. For other systems no transition was observed down to 1.4 K. In $U_{0.97}Np_{0.03}Pd_2Al_3$, the resistivity shows an increasing behavior with decreasing temperature below 7 K. Similar effects were already observed in other doped systems [15,16] and related to scattering due to alloying disorder, as reminiscent of the Kondo resistance minimum that occurs in metals containing small amounts of magnetic impurities.

3.2. Low range of An content, $0.05 \leq x \leq 0.1$

The resistivity curves obtained for a relatively low content of the dopants, Np (x_{Np}) and Pu (x_{Pu}), are shown in Fig. 2. At high temperatures the general features already observed in the previously discussed systems are still valid (see Table 2). However, a marked decrease of the position

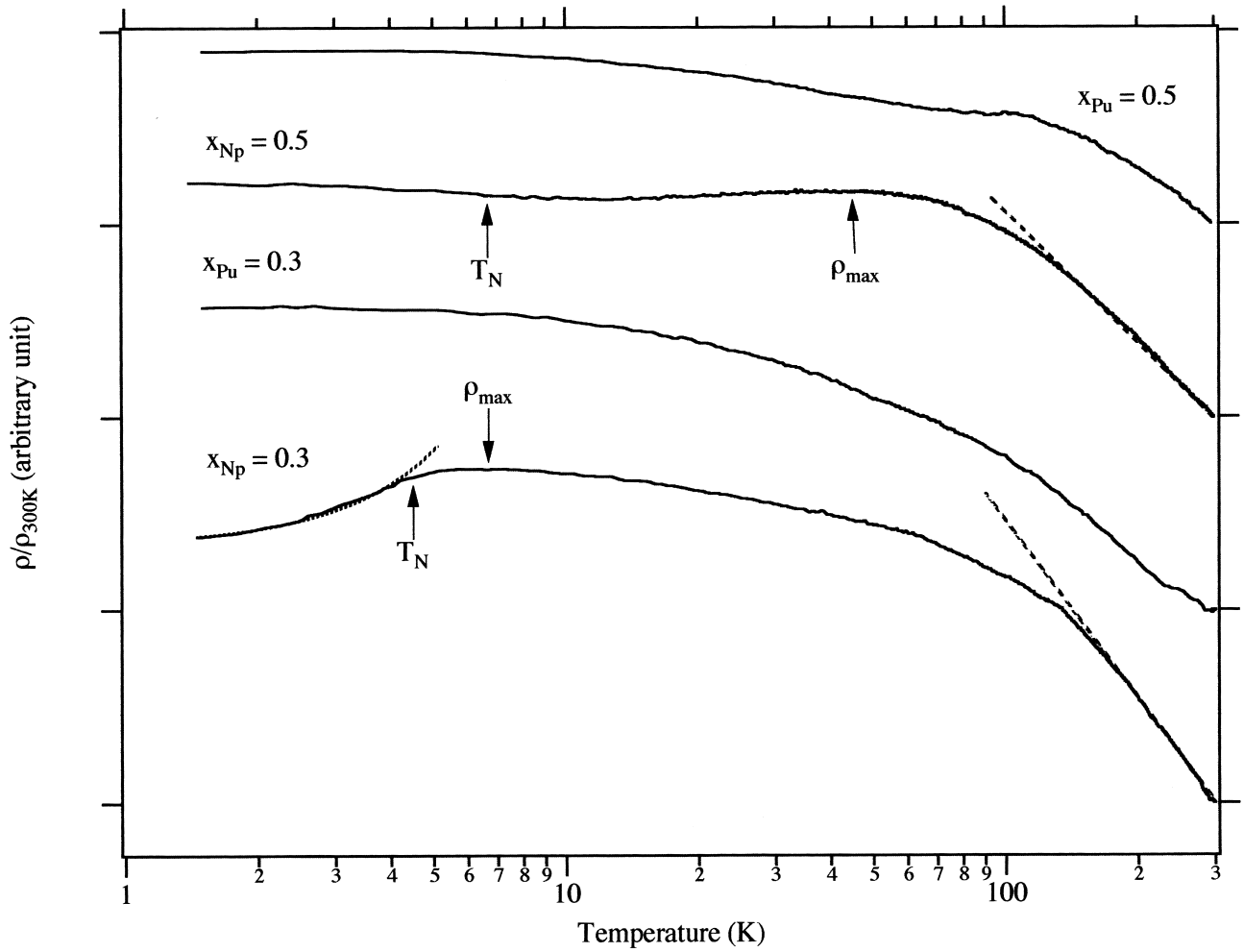

Fig. 3. Normalized resistivity $\rho/\rho_{300\ K}$ vs. a logarithmic scale of T, of $U_{1-x}An_xPd_2Al_3$ compounds. Curves are displaced for clarity. Arrows point out characteristic temperatures, as indicated in Table 1, and dashed lines show results of calculation as described in the text.

$T\rho_{max}$ of the maximum in resistivity arises. Even, for $U_{0.9}Pu_{0.1}Pd_2Al_3$ this maximum is sharper. It has been proposed that this type of maximum in $\rho(T)$ arises from the combined effect of CEF and Kondo interactions [6]. We may conclude that the effects of alloying on the distribution of crystal-field levels become sensitive for $x \geq 0.1$ and is maximum with Pu dopant.

At lower temperature, an abrupt decrease of the resistivity occurs below the ordering temperature, marked by a rupture in the slope (Fig. 2). Below 10 K, we could not achieve a reliable fit of the experimental data with an Eq. (2) type law. However, an excellent fit (dashed line) of the experimental data could be obtained using a non-gapped dispersion relation of the type:

$$\rho = \rho_0 + AT^2 \tag{3}$$

with the parameters listed in Table 2, reflecting spin fluctuation phenomena. We must underline the high value of the A parameter for 10% Pu-doped sample, suggesting an enhanced heavy-fermion type behavior.

3.3. Middle range of An content, $0.3 \leq x \leq 0.5$

For the middle range of Np- or Pu-content (30–50%), the resistivity curves obtained are completely different (Fig. 3). In the higher range of temperature, an increase of ρ with decreasing temperature is nevertheless a common feature.

The curves obtained for the Pu-doped samples are similar to these observed for their homologues Th-doped compounds [9]. At low temperature, below 50 K for $x_{Pu} = 0.3$ and below 40 K for $x_{Pu} = 0.5$, the variation of the resistivity is very close to linear in T. A similar behavior in Th-doped compounds was understood as the signature of non-Fermi-liquid properties [16,17].

$U_{0.7}Np_{0.3}Pd_2Al_3$ and $U_{0.5}Np_{0.5}Pd_2Al_3$ show a rounded maximum around 7 and 40 K, respectively, and look like curves of dilute Kondo impurity. Around 4.5 and 5.5 K, anomalies suggest the onset of a magnetic ordering as previously observed by Mössbauer spectroscopy [10,11]. Below the ordering temperature, $U_{0.7}Np_{0.3}Pd_2Al_3$ displays a decrease of ρ, with decreasing T, which can be well

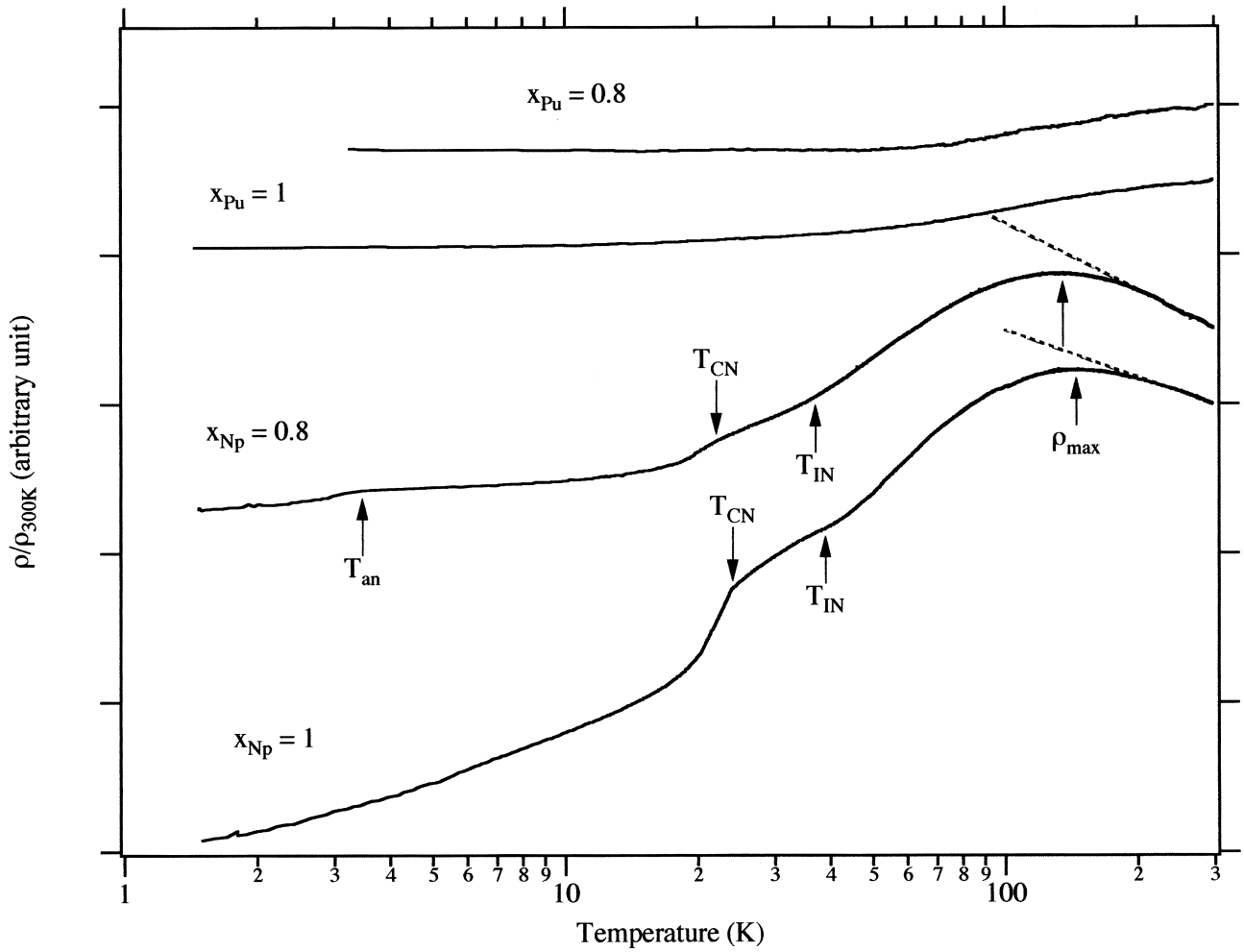

Fig. 4. Normalized resistivity $\rho/\rho_{300\ K}$ vs. a logarithmic scale of T, of $U_{1-x}An_xPd_2Al_3$ compounds. Curves are displaced for clarity. Arrows point out characteristic temperatures, as indicated in Table 1, and dashed lines show results of calculation as described in the text.

Table 2
Normalized values of the parameters used in the fit of the experimental data as indicated in the text

Compound	b/a	$\rho_0/\rho_{300\ K}$	$c/\rho_{300\ K}$	$\Delta/\rho_{300\ K}$	$A/\rho_{300\ K}$
UPd_2Al_3	0.101	0.061	0.060	27.4	0.0020
$U_{0.995}Np_{0.005}Pd_2Al_3$	0.100	0.062	0.082	27	0.0015
$U_{0.99}Np_{0.01}Pd_2Al_3$	0.104	0.132	0.058	25	0.0018
$U_{0.99}Pu_{0.01}Pd_2Al_3$	0.101	0.116	0.064	26.5	0.0019
$U_{0.97}Np_{0.03}Pd_2Al_3$	0.125	0.203	0.058	14	0.0012
$U_{0.92}Np_{0.08}Pd_2Al_3$	0.075	0.619	—	—	0.0025
$U_{0.9}Np_{0.1}Pd_2Al_3$	0.106	0.719	—	—	0.0034
$U_{0.9}Pu_{0.1}Pd_2Al_3$	0.139	0.522	—	—	0.0072
$U_{0.7}Np_{0.3}Pd_2Al_3$	0.106	1.269	—	—	0.0039
$U_{0.7}Pu_{0.3}Pd_2Al_3$	—	1.320	—	—	—
$U_{0.5}Np_{0.5}Pd_2Al_3$	0.093	1.247	—	—	—
$U_{0.5}Pu_{0.5}Pd_2Al_3$	—	1.784	—	—	—
$U_{0.2}Np_{0.8}Pd_2Al_3$	0.070	0.759	—	—	—
$U_{0.2}Pu_{0.8}Pd_2Al_3$	—	0.942	—	—	—
$NpPd_2Al_3$	0.060	0.415	—	—	—
$PuPd_2Al_3$	—	0.908	—	—	—

described according to a simple quadratic law (Eq. (3)), whereas $U_{0.5}Np_{0.5}Pd_2Al_3$ shows an almost linear increase. This increase may be first related to the partial frustration of the Np- and the U-moment due to the Np moment rotation out of the c-axis, as evidenced by Mössbauer spectroscopy [11].

3.4. High range of Np content, $0.9 \leq x \leq 1$

$NpPd_2Al_3$ orders initially at about 40 K (T_{IN}) in an incommensurate antiferromagnetic structure. Below 25 K (T_{CN}) the intensity of this phase is reduced in favor of the occurrence of a new commensurate antiferromagnetic magnetic ordering, which becomes the dominant phase [5]. The resistivity curves obtained for $U_{0.2}Np_{0.8}Pd_2Al_3$ and $NpPd_2Al_3$ are shown in Fig. 4. In the paramagnetic range, ρ exhibits a logarithmic T variation typical of a Kondo type behavior. The ordering temperature (T_{IN}) is assigned at 38 K, where a first anomaly in the curve is seen. Around 24 K (T_{CN}) a second anomaly is observed and related to occurrence of the second phase. By doping with 20% U

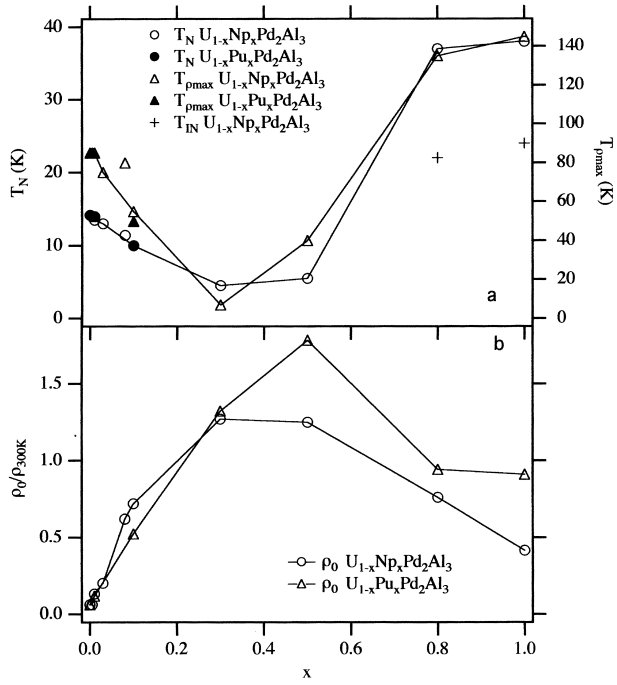

Fig. 5. Variation of some characteristic parameters as a function of the concentration of the An doping element.

($x_{Np}=0.8$), the general behavior of the compound remains almost unchanged. A slight decrease of the ordering temperatures (T_{IN} and T_{CN}) is nevertheless observed. At low temperature, the decrease of the resistivity with decreasing T is less pronounced, which may be due to disorder scattering. However, a third anomaly of an unknown origin is seen around 3 K. More experiments on this sample are necessary to clarify this last anomaly.

$PuPd_2Al_3$ is a non-magnetic system [4]. Its resistivity reveals a small decrease toward decreasing T, and below 150 K shows almost a linear variation. By doping with 20% U ($x_{Pu}=0.8$), the high-temperature behavior is unchanged. However, below 50 K its resistivity levels off to almost a constant value. Very few data are known for Pu ternary intermetallics and doped systems and, therefore, restrict the discussion on these systems.

To summarize and to get a better overview of the different observations reported in this paper we show in Fig. 5 the variation of some characteristics parameters as a function of the concentration of the An doping element. We see that for low content ($<30\%$) of doping with Np or Pu, these elements have nearly the same effects. At higher concentration Pu-doped samples do not order magnetically, whereas Np-doped samples display complicated features in the $0.3\leq x\leq 0.5$, and the properties of $NpPd_2Al_3$ seem to be almost unaffected by U-doping.

4. Conclusions

UPd_2Al_3–$NpPd_2Al_3$ and UPd_2Al_3–$PuPd_2Al_3$ are interesting systems where solid solutions are formed in the whole range of concentration. Moreover, substitution by Np or Pu adds a new dimension to doping effects as they contribute to an increase of the total number of 5f electrons. We have presented and summarized here the first characterization of their physical properties by resistivity measurements.

Very low Np content ($\leq 0.5\%$) decreases the temperature of the superconducting transition to 1.5 K. This suggests that a superconducting transition may be still observed below 1.4 K in Np- and Pu-doped samples at least for a content $\leq 1\%$. Further experiments of resistivity measurements at the mK range are necessary to investigate the influence of 5f element doping on the superconducting temperature. It is also interesting to note that, for An contents around 10%, the low temperature behavior seems to indicate a vanishing of the energy gap Δ observed in pure UPd_2Al_3 in favor of a spin fluctuation behavior with somehow enhanced heavy-fermion type properties. At higher contents in Np, our results corroborate the appearance of a complex magnetic competition between U and Np ions, whereas Pu cancels long-range magnetic correlations. The similar dependencies of T_N and $T_{\rho max}$ with regard to the content of doping Np or Pu, suggest that Kondo lattice effects and magnetic order are suppressed by the same mechanisms. Complementary studies of these systems, especially by neutron diffraction, are in progress.

Acknowledgements

The high-purity Np metal required for the fabrication of the compounds presented here, was made available through a loan agreement between Livermore National Laboratory and EITU, in the frame of a collaboration involving LLNL, Los Alamos Laboratory, and the US Department of Energy. The authors are pleased to express their thanks to G.H. Lander, S. Zwirner and J.C. Griveau for stimulating discussions.

References

[1] H.R. Ott, Z. Fisk, in: A.J. Freeman, G.H. Lander (Eds.), Handbook on the Physics and Chemistry of Actinides, vol. 5, Chap. 2, Elsevier Science, Amsterdam, 1987, p. 85.
[2] C. Geibel, C. Schank, S. Thies, H. Kitazawa, C.D. Bredl, A. Böhm, M. Rau, A. Grauel, R. Caspary, R. Helfrich, U. Alheim, G. Weber, F. Steglich, Z. Phys. B 84 (1991) 1.
[3] S. Zwirner, J.C. Spirlet, J. Rebizant, W. Potzel, G.M. Kalvius, C. Geibel, F. Steglich, Physica B 186,188 (1993) 681.
[4] A. Seret, F. Wastin, J.C. Waerenborgh, S. Zwirner, J.C. Spirlet, J. Rebizant, Physica B 206–207 (1995) 525.
[5] A. Hiess, P. Burlet, E. Ressouche, J.P. Sanchez, F. Bourdarot, F. Wastin, J. Rebizant, E. Suard, G.H. Lander, Phys. Rev. B 55(2) (1997) 1138.
[6] C. Geibel, C. Schank, F. Jährling, B. Bushinger, A. Grauel, T. Lühmann, P. Gegenwart, R. Helfrich, P.H.P. Reinders, F. Steglich, Physica B 199–200 (1994) 128.

[7] K. Ghosh, S. Ramakrishnan, Girish Chandra, Phys. Rev. B 47(130) (1993) 8305.
[8] S. Süllow, B. Ludoph, B. Becker, G.J. Nieuwenhuys, A.A. Menovsky, J.A. Mydosh, Phys. Rev. B 56(92) (1997) 846.
[9] Y. Dalichaouch, M.B. Maple, Physica B 199–200 (1994) 176.
[10] F. Wastin, S. Zwirner, A. Seret, J.C. Waerenborgh, A. Hiess, J. Fearon, E. Bednarczyk, J. Rebizant, J.P. Sanchez, Physica B 223(22) (1996) 211.
[11] S. Zwirner, J.C. Waerenborgh, F. Wastin, J. Rebizant, J.C. Spirlet, W. Potzel, G.M. Kalvius, Physica B 230–232 (1997) 80.
[12] F. Wastin, J. Rebizant, A.D. Stalios, C.T. Walker, this conference.
[13] Y. Dalichaouch, M.C. Andrade, M.B. Maple, Phys. Rev. B 46(13) (1992) 8671.
[14] N.H. Andersen, H. Smith, Phys. Rev. B 19 (1979) 384.
[15] A. Lopez de la Torre, P. Visani, Y. Dalichaouch, B.W. Lee, M.B. Maple, Physica B 179 (1992) 208.
[16] J.G. Park, S.B. Roy, B.R. Coles, J. Phys. Condens. Matter 6 (1994) 5937.
[17] M.B. Maple, M.C. de Andrade, J. Herrmann, Y. Dalichaouch, D.A. Gajewski, C.L. Seaman, R. Chau, R. Movshovich, M.C. Aronson, R. Osborn, J. Low Temp. Phys. 99(3/4) (1995) 223.